

УДК 535.361

**Rakhmatullaev I.A**

*DSc, prof.,*

*Alfraganus University*

*rakhmatullaev@afu.uz*

*<https://orcid.org/0000-0002-2348-7099>*

**Bunkin N.F**

*DSc, prof.,*

*N.E.Bauman Moscow State Technical University*

*nbunkin@mail.ru*

*<https://orcid.org/0000-0003-0802-6582>*

**Hoshimov Q.H**

*PhD student,*

*Samarkand State University named after Sharof Rashidov*

*<https://orcid.org/0009-0009-8304-2209>*

**Abdusattorov B.A**

*PhD student*

*Samarkand State University named after Sharof Rashidov*

*abdusattorovbobur86@gmail.com*

*<https://orcid.org/0009-0003-5262-4544>*

## **STUDY OF OPTICAL PROPERTIES OF MICROSTRUCTURED POWDERS OF DIAMOND, ZINC OXIDE AND TITANIUM DIOXIDE UNDER PULSE-PERIODIC LASER EXCITATION**

**Abstract.** The paper presents the results of an experimental study of the optical properties of microstructured powders of diamond, zinc oxide and titanium dioxide under the influence of pulsed-periodic laser radiation of nanosecond duration. The mechanisms of Raman scattering and photoluminescence spectrum formation in the studied samples at room temperature were investigated. The dependence of secondary radiation intensity on laser pulse energy density was established. It has been shown that microstructuring significantly affects the local distribution of the electromagnetic field, leading to an increase in nonlinear effects and a change in spectral characteristics. The results obtained can be used in the development of sensor systems, photocatalytic coatings, and functional optical materials.

**Keywords:** diamond, zinc oxide, titanium dioxide, powder, spectrum, microstructure, laser, luminescence, Raman scattering.

## IMPULS-DAVRIYLI LAZER NURI TA'SIRIDA MIKROSTRUKTURLANGAN OLMOS, RUX OKSIDI VA TITAN DIOKSIDI KUKUNLARINING OPTIK XUSUSIYATLARINI O'RGANISH

**Annatotsiya.** Ishda nanosekund davomiylikdagi impuls-davriyli lazer nurlanishi ta'sirida olmos, rux oksidi va titan dioksidi mikrotuzilishli kukunlarining optik xususiyatlarini eksperimental tadqiq qilish natijalari keltirilgan. Xona haroratida o'rganilgan namunalarning Raman sochilishi va fotolyuminessensiya spektrlarining shakllanish mexanizmlari o'rganilgan. Ikkilamchi nurlanish intensivligining lazer impulsi energiyasi zichligiga bog'liqligi aniqlangan. Mikrostrukturalash elektromagnit maydonning lokal taqsimlanishiga sezilarli ta'sir ko'rsatib, nochiziqli effektlarning kuchayishiga va spektral xarakteristikalarining o'zgarishiga olib kelishi ko'rsatilgan. Olingan natijalar sensor tizimlar, fotokatalitik qoplamalar va funksional optik materiallarni ishlab chiqishda qo'llanilishi mumkin.

**Kalitli so'zlar:** olmos, rux oksidi, titan dioksidi, kukun, spektr, mikrostruktura, lazer, lyuminesensiya, Raman sochilishi

## ИССЛЕДОВАНИЕ ОПТИЧЕСКИХ СВОЙСТВ МИКРОСТРУКТУРИРОВАННЫХ ПОРОШКОВ АЛМАЗА, ОКСИДА ЦИНКА И ДИОКСИДА ТИТАНА ПРИ ИМПУЛЬСНО-ПЕРИОДИЧЕСКОМ ЛАЗЕРНОМ ВОЗБУЖДЕНИИ

**Аннотация.** В работе представлены результаты экспериментального исследования оптических свойств микроструктурированных порошков алмаза, оксида цинка и диоксида титана при воздействии импульсно-периодического лазерного излучения наносекундной длительности. Изучены механизмы формирования спектров Рамановского рассеяния и фотолюминесценции изученных образцов при комнатной температуре. Установлены зависимости интенсивности вторичного излучения от плотности энергии лазерного импульса. Показано, что микроструктурирование существенно влияет на локальное распределение электромагнитного поля, приводя к усилению нелинейных эффектов и изменению спектральных характеристик. Полученные результаты могут быть использованы при разработке сенсорных систем, фотокаталитических покрытий и функциональных оптических материалов.

**Ключевые слова:** алмаз, оксид цинка, диоксид титана, порошок, спектр, микроструктура, лазер, люминесценция, Рамановское рассеяние.

### Introduction

The study of the interaction of pulsed laser radiation with dispersed media is of considerable interest for applied photonics and materials

science. Microstructured powders have a developed surface, high defect density, and pronounced particle shape anisotropy, which determines

the peculiarities of their optical response.

Wide-bandgap materials such as zinc oxide ( $E_g \approx 3.37$  eV) and titanium dioxide ( $E_g \approx 3.0$ – $3.2$  eV) are widely used in photocatalysis, sensor technology, and ultraviolet light sources. Diamond ( $E_g \approx 5.5$  eV) is characterised by high thermal conductivity, optical transparency and resistance to laser radiation.

The optical and luminescent characteristics of these items have been examined in many studies. Nonetheless, the mechanisms responsible for the generation of secondary radiation in finely dispersed and ultrafine dispersed media have not yet been sufficiently studied. Moreover, when powdered materials are irradiated with high-intensity pulses from pulsed lasers, their initial characteristics change significantly: the medium heats up intensely and photodestruction of the material may even occur [1–6].

The paper presents experimental data and results from the study of optical properties of microstructured powders of diamond, zinc oxide (ZnO) and titanium dioxide ( $\text{TiO}_2$ ) under pulse-periodic laser excitation.

### Experimental

Commercial diamond microcrystals were obtained by static compression at high temperature (1000–3000 °C) and ultra-high pressure (5–10 GPa) [5]. Ready-to-use ZnO and  $\text{TiO}_2$  micropowders from Sigma-Aldrich with a purity of 99% were used for the

study. The optical method, detailed in [3,6–8], was employed to excite and record the secondary radiation (SR) spectra. A copper vapour laser (CVL) line with a wavelength of  $\lambda = 510.6$  nm was used as the exciter, while the yellow line with  $\lambda = 578.2$  nm was excluded by filtering. The average radiation power reaches 10 W, the radiation is formed in pulse mode with a high repetition rate of  $10^4$  Hz, and the pulse duration is 20 ns, which provides a peak power of up to  $10^5$  W. The radiation is generated in a pulsed mode at a high repetition rate ( $10^4$  Hz) with short pulses lasting 20 ns, which provides a peak power of  $10^5$  W. Neutral light filters (NF) were used to calibrate the intensity of two-photon excited luminescence (TPEL) spectra. The microparticle samples were tightly packed between flat parallel quartz cuvette windows. The spectrophotometry cuvettes were made of “KU” quartz glass. The layer thickness was 1 mm. The resolution of the spectrum recording in the measured wavelength range was 0.1 nm. The sizes of the micropowders studied were as follows: synthetic microcrystalline diamond with an average particle size of 5  $\mu\text{m}$ ; ZnO powder (average particle size 3  $\mu\text{m}$ ); anatase  $\text{TiO}_2$  powder (average particle size 10  $\mu\text{m}$ ).

The measurements were carried out at room temperature. Single-photon-excited luminescence (SPEL) spectra were recorded using the second optical harmonic (SOG) of the green line (510.6 nm) of laser radiation

in copper vapour, which corresponds to a wavelength of  $\lambda = 255.3$  nm [7]. The high intensity of the laser radiation ensures efficient generation of the second harmonic and total frequency conversion due to nonlinear optical crystals of the  $BaB_2O_4$  type. The radiation from the active element of the laser, operating in an unstable resonator mode, was directed to the  $BaB_2O_4$  crystal through a lens with an increased focal length. The visible laser radiation was blocked by an absorbing filter located after the  $BaB_2O_4$  crystal.

## Results and Discussion

### Diamond

Figure 1 shows the SPEL spectra of diamond micropowders of various sizes when excited by the second optical harmonic of CVL ( $\lambda_{exc}=255.3$  nm). The spectra were recorded under

identical excitation and recording conditions. This fact excludes the possibility of differences caused by the methodology. As can be seen from the figure, the SPEL spectrum of these samples (curves 1-3) is in the range of 300-530 nm and represents a broad band with two maxima in the region of 420 and 460 nm. In addition, a weak band is observed in the short-wave region of the spectrum ( $\lambda=360$  nm). For diamond particles with an average size of 10  $\mu\text{m}$ , this band peak is clearly visible. For diamond, the energy of two green quanta or the energy of the second harmonic from the green laser line on copper vapour  $\lambda_{exc}=255.3$  nm (4.8 eV) does not exceed  $E_g$ , i.e.  $E_{exc} < E_g$  ( $E_g=5.4-5.5$  eV).

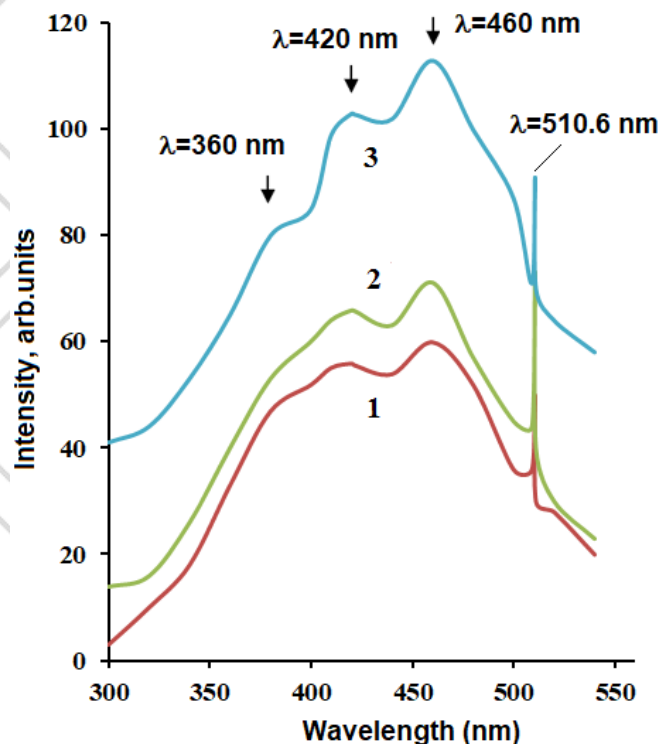


**Figure 1.** SPEL spectra of diamond micropowders of various sizes when excited by the second optical harmonic of a copper vapour laser ( $\lambda_{exc}=255.3$  nm): (1) -  $d_{mean}=0.5$   $\mu\text{m}$ ; (2) -  $d_{mean}=1$   $\mu\text{m}$ ; (3) -  $d_{mean}=10$   $\mu\text{m}$ . Power density of the exciting radiation  $I_{exc} \sim 10^7$  W/cm<sup>2</sup>.

The results showed that in our studies, photoluminescence in diamond occurs with the participation of defects in the powder [5,6]. It is known that the bands in the 410–460 nm range in the SPEL spectrum are caused by electronic transitions between the doubly degenerate excited state ( $E_1$ ) and the main non-degenerate state ( $A_1$ ) of the N3 defect in the SPEL spectrum of natural diamonds. The weak maximum at  $\lambda=380$  nm in the SPEL spectra can be attributed to the N2 defect. In addition, the close proximity and similarity of the spectral line obtained in our experiment to the known line corresponding to the N2 defect in a large diamond allows us to conclude that the observed line belongs to this type of defect. The N3 centre is always accompanied by the N2 centre [9].

The Raman scattering spectra of diamond micropowders of various

sizes when excited by the green line of the CVL ( $\lambda_{exc}=510.6$  nm) are shown in Figure 2. Practically all samples show a feature at  $\nu=1332$   $\text{cm}^{-1}$ , corresponding to the fundamental vibration of the diamond lattice. The registration of a narrow line at this frequency confirms the presence of the diamond crystalline phase in the samples under study. However, the spectra show a luminescent background throughout the entire TPEL-related spectral region. As the particle size increases, the continuous luminescence background decreases sharply and the intensity of Raman scattering at the fundamental mode of  $1332$   $\text{cm}^{-1}$  relative to the background increases. As can be seen from the results, the intensity of  $1332$   $\text{cm}^{-1}$  increases with increasing average diamond particle size.

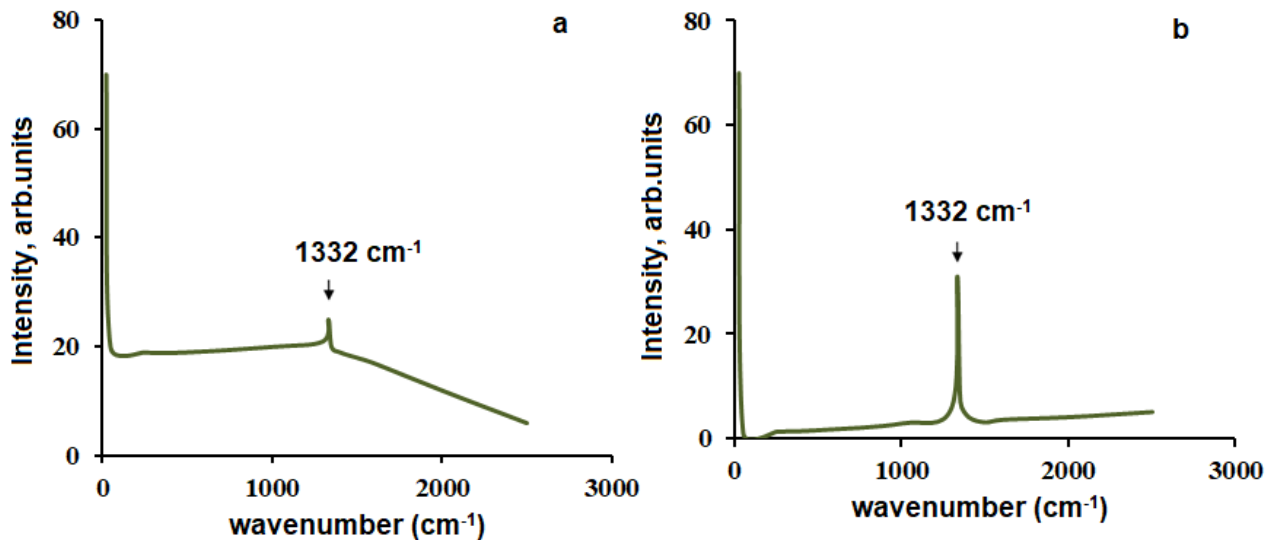
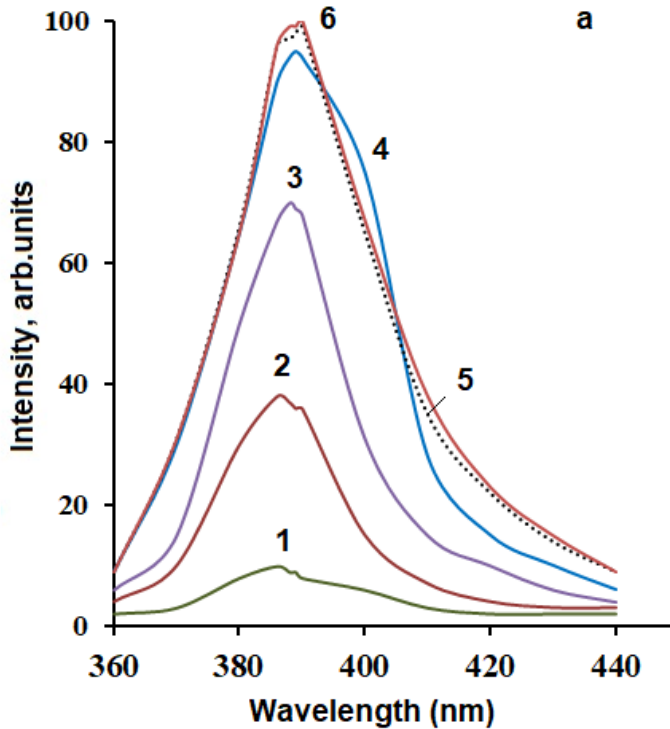


**Figure 2.** Raman scattering spectra of diamond micropowders of various sizes when excited by a green laser line on copper vapour ( $\lambda_{\text{exc}}=510.6$  nm): (a) -  $d_{\text{mean}}=0.5$   $\mu\text{m}$ ; (b) -  $d_{\text{mean}}=10$   $\mu\text{m}$  ( $I_{\text{exc}} \sim 10^5$  W/cm<sup>2</sup>).

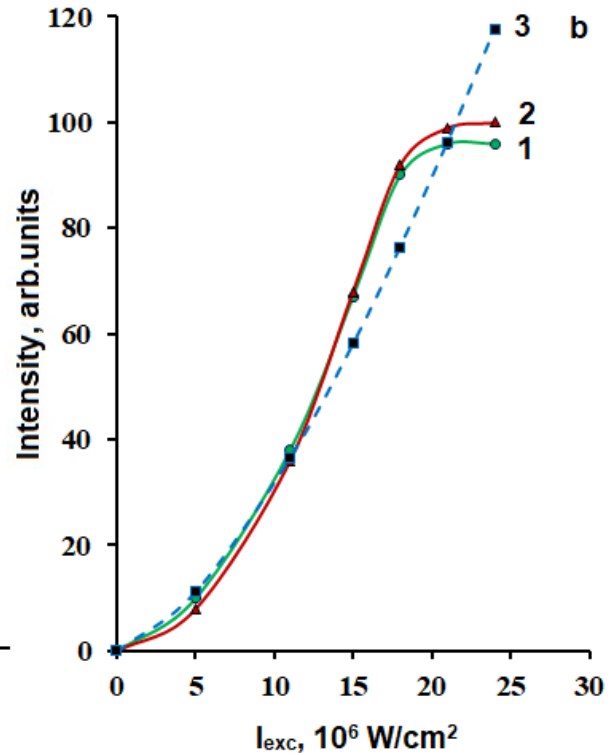
### Zinc oxide

Figure 3a shows the SPEL spectra of ZnO microcrystals obtained at various intensities of the excitation radiation ( $\lambda_{\text{exc}} = 255.3$  nm). At low excitation intensity, the SPEL spectrum exhibits a maximum at around 386 nm (curves 1 and 2). In semiconductor materials with low concentrations of impurities and defects, excitation at high intensities leads to radiative recombination of the free excitons. saturation of the excitation intensity occurs, and in this context, the following aspect of the large-scale annihilation of free excitons is of

particular interest: the possibility of obtaining stimulated emission arises [9]. It is well known that free excitons do not undergo an inversion distribution, whereas in photon and phonon emission by excitons inversion arises automatically. When the excitation intensity exceeds  $1.5 \times 10^6$  W/cm<sup>2</sup> (curves 3–5), a narrowing of the exciton luminescence line is observed, and its intensity increases non-linearly with further increases in the excitation intensity. Furthermore, the SPEL band narrows and the peak of this spectral intensity shifts into the longer-wavelength region by up to 4 nm.



**Figure 3a.** SPEL spectra of ZnO micropowder ( $d_{\text{mean}} = 3 \mu\text{m}$ ) obtained at different intensities of stimulating radiation: (1) -  $I_{\text{exc}} = 5$ ; (2) -  $I_{\text{exc}} = 11$ ; (3) -  $I_{\text{exc}} = 15$ ; (4) -  $I_{\text{exc}} = 18$ ; (5) -  $I_{\text{exc}} = 21$ ; (6) -  $I_{\text{exc}} = 24$ . ( $I_{\text{exc}} \sim 10^6 \text{ W/cm}^2$ ).



**Figure 3b.** The dependence of the SPEL intensity ( $I$ ) on the excitation radiation intensity ( $I_{\text{exc}}$ ) for ZnO microcrystals ( $d_{\text{mean}} = 2 \mu\text{m}$ ). The line (1) corresponds to a wavelength of 386 nm; (2) -  $\lambda = 390 \text{ nm}$ . (3) - the theoretical dependence in accordance with the law  $I \approx I_{\text{exc}}^{1.5}$ .

Under our experimental conditions ( $I_{\text{exc}} \approx 10^6 \text{ W/cm}^2$ ), a power-law dependence with an exponent  $\alpha \approx 1.5$  is observed for the ZnO microstructures (Figure 3a, 3-line), which corresponds to the  $\alpha = 1.5 \pm 0.2$  value found for bulk ZnO in [10]. At high intensities, the growth of SPEL intensity slows down, which may be caused both by heat effects and by the formation of defects through photolysis and thermodestruction. A similar trend was observed for monocrystalline ZnO and quantum dots in [11]. The absence of

visible SPEL in our ZnO samples indicates a low concentration or absence of oxygen defects [10-12] and the high purity of the ZnO powders studied.

### Titanium dioxide

Figure 4 shows the Raman scattering spectra of  $\text{TiO}_2$  micropowders obtained in cuvettes of various designs under identical recording conditions. Curve 1 corresponds to a cylindrical cuvette with a relatively large volume (cuvette diameter 18 mm), and curve 2 corresponds to a so-called resonator

cuvette with a capillary diameter of 3 mm. An OG-1 light filter was installed in front of the monochromator slit, attenuating the laser excitation line ( $\lambda_{exc}=510.6$  nm) 100 times while allowing full transmission of the Raman

scattering signal at a distance of 800  $cm^{-1}$  from the excitation line. As can be seen from this figure, the Raman scattering signal in the resonator cuvette is almost 1000 times greater than in a cylindrical cuvette with a large diameter.

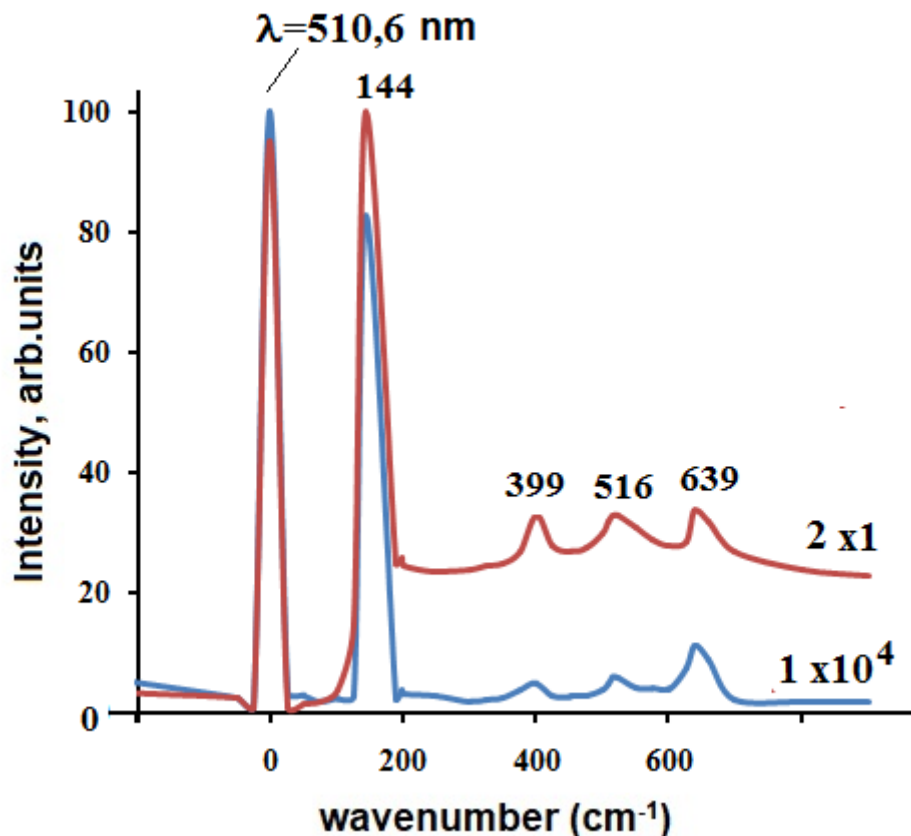


**Figure 4.** Raman scattering spectra of  $TiO_2$  micropowders ( $d_{mean}=10$   $\mu m$ ) in a cylindrical cuvette (1) and in a resonator cuvette (2) ( $I_{exc}\sim 10^5$   $W/cm^2$ ).

Thus, in photon traps, the intensity of Raman scattering of  $TiO_2$  micropowders at the cuvette outlet increases significantly (Fig. 4): a significant increase in the relative intensity of Raman scattering is observed compared to the intensity of the excitation line (combination opalescence mode). This is explained by a significant increase in the total path length that the excitation photon travels in the studied

substance due to multiple reflections from the trap walls and scattering on the inhomogeneities of the medium.

Figure 5 illustrates the SPEL spectra of  $TiO_2$  micropowders obtained by exciting them with a 255.3 nm laser line on copper vapour (curve 1). For comparison, the TPEL spectra of  $TiO_2$  micropowders at room temperature (curve 2) are also shown here, when excited by a green line (510.6 nm) laser

on copper vapour. These spectra were recorded under the same excitation and recording conditions. Comparisons of the experimental results show that the SPEL and TPEL spectra differ in intensity, shape and position. As can be seen from the figure, these spectra (curves 1–2) are in the range of 360–560 nm and represent a fairly narrow single line, while the SPEL spectrum has a maximum in the region of 430 nm (2.90 eV). The maximum of the TPEL spectrum is shifted to the short-wave region by 3 nm relative to the SPEL spectrum with a peak in the region of  $\lambda=427$  nm (2.91 eV). It should be noted that single-photon and two-photon photoluminescence spectra carry different information. For example, in the dipole approximation, two-photon transitions are allowed between states of the

same parity, while single-photon transitions are allowed between states of different parity. These maxima have also been observed in the works of other authors: they can be attributed to the recombination of free excitons, as they are often observed in various TiO<sub>2</sub> structures: single crystals [13,14], nanoparticles [15] and colloidal nanoparticles [16]. The relatively high intensity of the photoluminescence signal is associated with the powder placed in the micro-resonator cuvette. In an optical micro-resonator, the nano-/microstructure itself and the material of the device (cell) can serve as an amplifying medium. As a result, fairly intense photoluminescence signals can be obtained at the output and mini lasers operating at room temperature can be created [17,18].

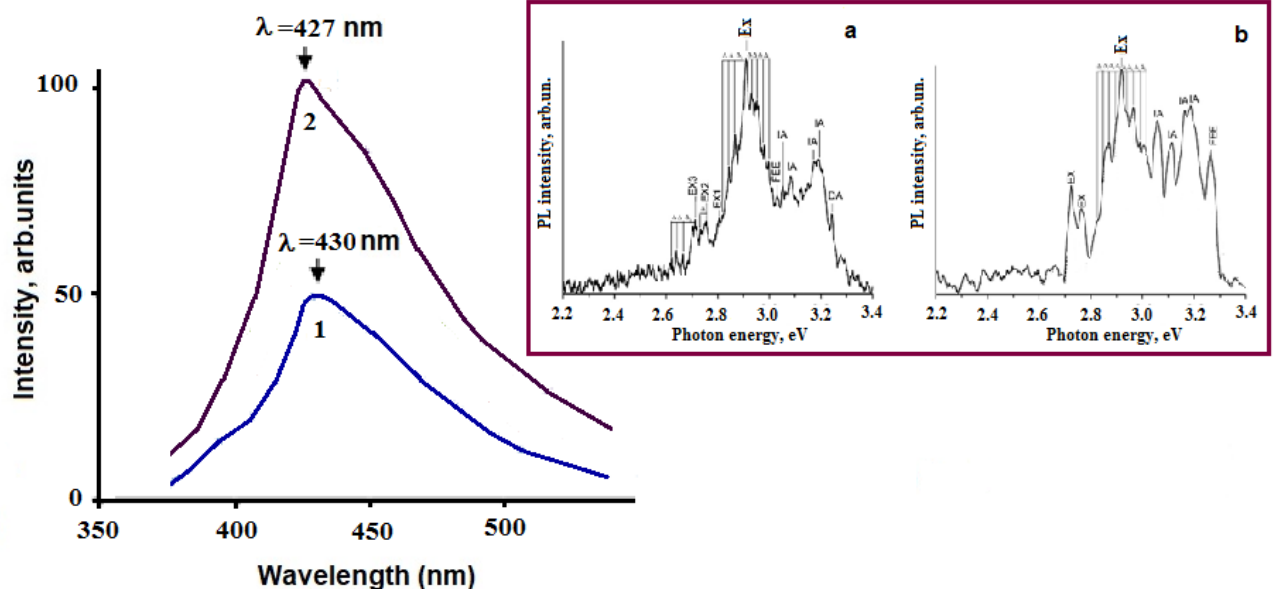


**Figure 5.** 1) - SPEL spectrum of TiO<sub>2</sub> micropowders when excited by ultraviolet radiation ( $\lambda_{exc}=255.3$  nm); 2) - TPEL spectrum of TiO<sub>2</sub> micropowders when excited by two green quanta ( $E=2\hbar\omega=4.8$  eV). The average size of the particles studied is  $d_{mean}=10$   $\mu$ m ( $I_{exc} \sim 10^7$  W/cm<sup>2</sup>). The inset shows the photoluminescence spectra of

rutile nanostructures at T=300 K (A) and the photoluminescence spectra of anatase nanostructures at T=300 K (B), obtained in [15].

Thus, analysis of the literature shows that the insignificant presence of silicon and aluminium impurities in TiO<sub>2</sub> samples does not affect the formation of the photoluminescence peak in the 2.90-2.91 eV range, which is consistent with our experimental studies. The observed photoluminescence maxima in the 427–430 nm region in TiO<sub>2</sub> micropowders can be attributed to the recombination of free excitons.

### Conclusion

A method has been developed for studying the secondary radiation of

microstructured powders under pulsed periodic laser excitation. The superlinear dependence of ZnO luminescence intensity on laser power density has been experimentally confirmed. Weak Raman scattering signals have been recorded in diamond and TiO<sub>2</sub> microstructures. The results obtained can be used in the creation of laser sensors, photocatalytic systems, and nonlinear optical converters.

### References

1. Abduev, A.Kh. et al. Ultraviolet Luminescence of Zinc Oxide Epitaxial Layers under One- and Two-Photon Excitations. *Kvantovaya elektronika*, 1978, Vol.5, No.1. – pp.206–208 (in Russian).
2. Sokolovskiy, M.I. Secondary Emission of Nanocrystalline Zinc Oxide under Laser Excitation. PhD diss. Ulyanovsk: *Ulyanovsk State University*, 2006, 127 p. (in Russian).
3. Rakhmatullaev, I.A., Bunkin, N.F. & Davronov, M.K. Effect of Raman Opalescence on Titanium Dioxide Micropowders Under Pulse-Periodic Laser Excitation. *Journal of Applied Spectroscopy*, 2025, Vol. 91. – pp.1256–1260. <https://doi.org/10.1007/s10812-025-01846-9>
4. Bourezgue, A., Kasem, I., Daoudi, M. et al. Influence of Gamma-Irradiation on Structural, Optical and Photocatalytic Performance of TiO<sub>2</sub> Nanoparticles under Controlled Atmospheres. *Journal of Electronic Materials*, 2020, Vol.49, pp. 1904-1921. <https://doi.org/10.1007/s11664-019-07887-z>
5. Gorelik, V., Skrabatun, A. & D. Bi. Raman Scattering of Light in Diamond Microcrystals. *Crystallography Reports*, 2019, Vol.64, pp. 428-432. <https://doi.org/10.1134/S106377451903009X>
6. Rakhmatullaev, I.A., Gorelik, V.S., Muminov, R.A. at al. Photoluminescence and Raman Spectra of Diamond Micropowders Placed in Photon Traps. *Scientific-technical journal*, 2021, Vol. 4, No.1. – pp. 46–53. (in Russian).
7. Gorelik, V.S., & Rakhmatullaev, I.A. Spectral and temporal characteristics of the photoluminescence of cotton upon laser UV excitation. *Journal of applied spectroscopy*, 2004, Vol. 71, No.5. – pp.661–664.

- <https://doi.org/10.1023/b:japs.0000049624.75960.86>
8. Rakhmatullaev, I., Bunkin, N., Davronov, M., et al. Microwave Synthesis and Study of Morphology, Structure and Luminescent Properties of Zinc Oxide Microstructures. *Journal of Physical Science*, 2025, Vol.36, No.1. – pp. 27–36. <https://doi.org/10.21315/jps2025.36.1.3>
  9. Kaiser W., Bond W. Nitrogen, a Major Impurity in Common Type I Diamond // *Physical Review*, 1959, Vol. 115, No. 4. – pp. 857-863.
  10. Rakhmatullaev, I.A., Tcherniega, N.V., Davronov, M.Kh. et al. Raman Scattering Spectra in Zinc Oxide Microstructures Placed in Photon Traps. International Conference on Advanced Laser Technologies (ALT-22), 2022, – pp. 188.
  11. Fonoberov, V.A., Alim, Kh.A., Balandin, A.A., et al. Photoluminescence Investigation of the Carrier Recombination Processes in ZnO Quantum Dots and Nanocrystals. *Physical Review B*, 2006, Vol.73. – pp.165317. <https://doi.org/10.1103/PhysRevB.73165317>
  12. Burakov, V.S., Tarasenko, N.V., Nevar, E.A., et al. Morphology and Optical Properties of Zinc Oxide Nanostructures Synthesized By the Methods of Thermal and Discharge Sputtering. *Technical Physics*, 2011, Vol. 56, No.2. – pp. 245-253. <https://doi.org/10.1134/s1063784211020071>
  13. Tang H., Berger H., Schmid P.E., et al. Photoluminescence in TiO<sub>2</sub> Anatase Single Crystals. *Solid State Communications*, 1993, Vol.87. – pp.847–850.
  14. Haart L.G., Blasse G. The Observation of Exciton Emission from Rutile Single Crystals. *Solid State Chemistry*, 1986, Vol.61. – pp.135–137.
  15. Kernazhitsky L., Shymanovska V., Gavrilko T. et al. Room Temperature Photoluminescence of Anatase and Rutile TiO<sub>2</sub> Powders. *Journal of Luminescence*, 2014, Vol.146. – pp.199–204. <https://doi.org/10.1016/j.jlumin.2013.09.068>
  16. Serpone N., Lawless D., Khairutdinov R. Size Effects on the Photophysical Properties of Colloidal Anatase TiO<sub>2</sub> Particles: Size Quantization versus Direct Transitions in This Indirect Semiconductor? *Journal of Physical Chemistry*, 1995, Vol.99. – pp.16646–16654.
  17. Rakhmatullaev, I.A., Tursunkulov, O.M., Gusev, A.L. et al. Morphological, Structural and Optical Properties of Titanium Dioxide Micropowders. *International journal "Alternative Energy and Ecology"*, 2021, No. 4-6. – pp. 126-138 (in Russian) <https://doi.org/10.15518/isjaee.2021.04-06.126-138>.
  18. Gargas D.J., Toimilmolaes M.E., Yang P. Imaging Single ZnO Vertical Nanowire Laser Cavities Using UV-laser Scanning Confocal Microscopy. *Journal of the American Chemical Society*, 2009, Vol.131. – pp.2125-2127. <https://doi.org/10.1021/ja8092339>